

國立交通大學

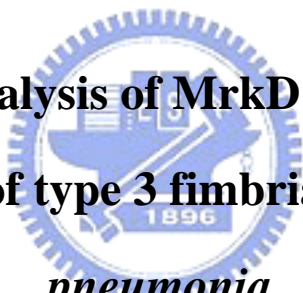
生物科技研究所

碩士論文

克雷白氏肺炎桿菌第三型纖毛組成蛋白 MrkD 與

MrkF 之功能探討

**Functional analysis of MrkD and MrkF, the
components of type 3 fimbriae in *klebsiella
pneumonia***



研究生：廖心瑋

學號：9328508

指導教授：彭慧玲 博士

中華民國 九十五年 七月

中文摘要

本實驗室在過去的研究中，將 17 株克雷白氏肺炎桿菌腦膜炎臨床分離株基因序列加以分析，並定出四種第三型纖毛黏附蛋白的變異型，分別命名為 MrkDv1, MrkDv2, MrkDv3, MrkDv4。將帶有不同黏附蛋白變異型的第三型纖毛分別表現在大腸桿菌 JM109 中，發現帶有 MrkDv3 黏附蛋白的纖毛具有最高的膠原蛋白黏附能力以及紅血球凝集能力。比較這四種黏附蛋白的胺基酸序列發現 MrkDv3 具有一段與其他三種黏附蛋白顯著不同的胺基酸序列位於第 120 到第 140 個胺基酸之間，顯示出此段胺基酸序列似乎與 MrkDv3 的高黏附能力相關。此外，基因重組大腸桿菌 HB101[pmrkABCF]與 HB101[pmrkABCD]皆能產生纖毛，顯示 MrkF 可能參與纖毛組裝過程。本實驗製作三種不同長度的 MrkDv3 截短蛋白分別帶有前 170 個胺基酸(MrkDv3NL)、前 150 個胺基酸(MrkDv3N)以及前 120 個胺基酸(MrkDv3NS)。不可溶性重組蛋白大量表現於重組大腸桿菌中並可藉由蛋白質電泳觀察出來。經由尿素處理加以純化而得的重組蛋白 dMrkDv3N 可以抑制帶有 pmrkABCDv3F 重組質體的大腸桿菌對第四型膠原蛋白的黏附力。此外，透過西方墨點法以及穿透式電子顯微鏡的觀察顯示 MrkF 是第三型纖毛的組成分子並且與調控纖毛長度有關。利用共沉澱分析進一步證實 MrkF 與 MrkA 於纖毛之中相互連結並且透過膠原蛋白黏附測試、生物膜形成測試、以及細菌聚集測試證實 MrkF 參與調控第三型纖毛的生物活性。

Abstract

Our previous analysis of type 3 fimbriae in 17 *Klebsiella pneumoniae* meningitis isolates has identified four type 3 fimbrial adhesin variants namely MrkDv1, MrkDv2, MrkDv3, and MrkDv4. The recombinant *Escherichia coli* JM109 displaying type 3 fimbriae with *mrkDv3* allele exerted the highest level of activity in collagen binding and mannose resistant hemagglutination. Sequence comparison with the other three variants revealed a most variable region from Gly₁₂₀ to Gln₁₄₀, suggesting a responsible sequence for the strongest adhesion activity. In addition, the recombinant *E. coli* HB101[pmrkABCF] expressed fimbriae as well as *E. coli* HB101[pmrkABCD] indicating the involvement of MrkF in fimbriation. In the study, the recombinant clones expressing with three truncated forms of MrkDv3 including MrkDv3_{1-170aa} (MrkDv3NL), MrkDv3_{1-150aa} (MrkDv3N), and MrkDv3_{1-120aa} (MrkDv3NS) were generated. Overexpression of all the recombinant proteins could be observed in *E. coli* BL21(DE3), however, appeared to be insoluble. Purification via urea denaturalization of the inclusion body was carried out and the purified protein MrkDv3N was shown to be able to inhibit the collagen binding activity of *E. coli* JM109[pmrkABCDv3F]. Moreover, analysis using western blotting hybridization, transmission electronic microscopy (TEM) with anti-MrkA and anti-MrkF sera demonstrated that MrkF is a component of type 3 fimbriae and likely a regulator for the length of the fimbriae. Co-immunoprecipitation analysis with anti-MrkF and anti-MrkA antibodies has proved an interaction of MrkA and MrkF. Finally, the assessment by the assays of collagen binding, biofilm formation, and autoaggregation, also showed that MrkF likely plays a regulatory role in the activity of type 3 fimbriae.

致謝

碩士班兩年，真正開啟了我的研究生涯，回想這兩年的生活，並不能稱得上順利，歷經大大小小的實驗瓶頸、試了各種方法卻無法克服的實驗困難，好幾次沮喪不已，真正嚐到了研究的本質-“實驗總是充滿了意外！”。值得慶幸的是，這兩年的生活並不算太苦悶，因為在我身邊有一個很好的老師-彭老師，老師嚴格卻不嚴厲，對我們的實驗不順不但不會嚴厲責備，取而代之的是不厭其煩的和我們討論，讓我非常感激，也從老師身上學到了許許多多，包括實驗的邏輯思考以及處事態度，相信會讓我一生受用不盡。感謝口試委員張晃猷老師以及楊昀良老師給我寶貴的建議與指教，使得這本論文更加完整。

此外，也很感激我的爸爸媽媽，他們圓融並樂觀積極的人生態度改變了我對事情的看法也轉化了負面的情緒。姐妹淘COCO，小毛，吳佳佳，更是提供我無數的歡樂，讓我不畏懼面對挑戰。當然，實驗室的戰友們，和我共渡了兩年的美好時光，感謝可愛又溫柔善良的丸子，在實驗上給我很大的幫助、直率的小新是很好的談話對象，還有有趣的靖婷學姊、健誠學長，以及細心盡責的智凱、熱心助人的育聖，很適合拍美食廣告的登魁、格維、朝陽和很有耐心的偉昌，有你們的幫助與陪伴，讓我的碩班生活變得多彩多姿，充滿歡笑！

最後更要感謝貼心的國領對我的照顧與支持，讓我可以實驗上衝刺無後顧之憂！謝謝所有關心我的人，因為你們，我才能快樂的渡過碩士生涯！

Contents

中文摘要.....	i
Abstract.....	ii
致謝.....	iii
Contents.....	iv
List of tables and figures.....	vi
Abbreviation.....	vii
Introduction.....	1
1. Clinical importance of <i>Klebsiella pneumoniae</i>	1
2. Adherence properties.....	1
2.1 Type 1 fimbriae.....	2
2.2 Type 3 fimbriae.....	3
3. Pilus biogenesis.....	4
4. Specific aims.....	5
Materials and methods.....	7
1. Strains, plasmids and growth conditions.....	7
2. Recombinant DNA technology- MrkD and MrkF clones.....	7
3. Protein expression and purification.....	8
4. Generation of anti- MrkF and anti MrkD antibody.....	9
5. Electron microscopy.....	10
6. Purification of type 3 fimbriae.....	10
7. Co-immunoprecipitation.....	11
8. Immunoblot analysis.....	11
9. Collagen binding assay.....	12

10. Biofilm formation assay.....	12
11. Autoaggregation assay.....	13
Results.....	14
1. Overexpression and purification of MrkD and MrkB recombinant proteins.....	14
2. Analysis of the purified dMrkDv3N in competition assay.....	15
3. MrkF is a component of type 3 fimbriae.....	16
4. MrkF influences the fimbriation of the recombinant <i>E. coli</i>	17
5. Assessment of the activity of the recombinant type 3 fimbriae.....	17
Discussions.....	19
1. Solubility improvement of the recombinant proteins.....	19
2. Localization of MrkF	19
3. Functional analysis of MrkF.....	20
References.....	22
Tables.....	29
Figures.....	33



List of tables and figures

Table 1. Bacteria strains used in this study.....	29
Table 2. Plasmids used and constructed in this study.....	30
Table 3. Primers used in this study.....	32
Fig. 1 Amino acid sequence alignment of the MrkD variants.....	33
Fig. 2 Amino acid sequence alignment of MrkA and MrkF.....	34
Fig. 3 Physical map of the recombinant proteins prepared in this study.....	35
Fig. 4 SDS-PAGE analysis of the recombinant proteins.....	36
Fig. 5 Competition assay.....	37
Fig. 6 Western blotting analysis of the recombinant <i>E. coli</i> displaying type 3 fimbriae...38	
Fig. 7 Western blotting analysis of the purified type 3 fimbriae.....	39
Fig. 8 Co-immunoprecipitation.....	40
Fig. 9 Electron micrographs of the anti-MrkF immuno-gold labeled pili.....	41
Fig. 10 Electron micrographs of the recombinant <i>E. coli</i>	42
Fig. 11 Collagen binding activity of the recombinant <i>E. coli</i>	43
Fig. 12 Biofilm formation of the recombinant <i>E. coli</i>	44
Fig. 13 Autoaggregative phenotypes.....	45

Abbreviation

APS	ammonium persulfate
BCIP	5-bromo-4-chloro-3-indolyl phosphate
bp	Base pair (s)
EDTA	<i>N,N,N,N'</i> -ethylenediaminetetraacetate
GCAA	glycerol cassamino acid
HA	hemagglutination
HECM	Human extracellular matrix
IPTG	isopropyl- β -D-thio-galactopyranoside
kDa	kiloDalton (s)
LB	Luria-Bertani broth
Man 1	monomannose
Man 3	trimannose
MR	Mannose resistance
NBT	nitro blue tetrazolium chloride
PBS	phosphate buffer saline
PBST	phosphate buffer saline-Tween 20
PCR	polymerase chain reaction
PVDF	polyvinylidene fluoride
rpm	revolution per minute
SDS-PAGE	sodium dodecyl sulfate-polyacrylamid gel electrophoresis
TEM	Transmission electronic microscopy
TEMED	<i>N, N, N', N'</i> - tetramethylethyl -enediamide
UPEC	uropathogenic <i>E. coli</i>

Introduction

1. Clinical importance of *Klebsiella pneumoniae*

Klebsiella pneumoniae is an opportunistic pathogen that attacks immunocompromised patients who are hospitalized and suffer from severe underlying diseases, such as chronic pulmonary obstruction or diabetes mellitus (1). In addition, the bacterial infections could lead to complicated urinary tract infections, septicemia and pneumonia in the elderly or in patients who have predisposing factors such as urinary catheters or primary infections caused by other microorganisms (2). It has been shown recently that the bacteria also cause meningitis which is mostly benign with the bacterial acquisition from nasopharyngeal colonization, a major reservoir of *K. pneumoniae* infections (3, 4). The virulence factors of *K. pneumoniae* identified including copious amounts of an acidic polysaccharide capsule (CPS) (5), lipopolysaccharides, iron acquisition systems and several distinct types of adherence factors (6). The adhesive molecules, including type 1 and type 3 fimbriae (7), KPF28 (8), and a nonfimbrial adhesin, CF29K (9) are believed to be responsible for *K. pneumoniae* to colonize respiratory and urinary epithelia.

2. Adherence properties

Adherence of bacteria to the epithelial cell of host is the first step during infection and the process is generally carried out by fimbriae, which are filamentous organelles exposed outside the lipopolysaccharide and capsular polysaccharide layers of the cell envelope (10). The fimbriae are built of the monomers of major structural protein pilin and on the tip with adhesin subunits usually of lectin properties (11). The fimbria-associated adhesins allow bacterial attachment to epithelial receptors of host and facilitate colonization of uroepithelial cells (12). Under different environments, *K.*

pneumoniae commonly produce type 1 fimbriae and type 3 fimbriae to achieve its colonization (13).

2.1. Type 1 fimbriae

Type 1 fimbriae are heteropolymeric fibers produced by all members of the *Enterobacteriaceae* family (14). They are required for bacterial attachment to mannose units of the glycoprotein receptor uroplakin Ia on the surface of urinary epithelium cells, and characterized by their ability to mediate mannose-sensitive agglutination of guinea pig or fowl erythrocytes (15). Approximately 70% of the uropathogenic *E. coli* strains carrying a minor mutation enhanced the lectin ability to recognize monomannose (Man 1), while 80% of the *E. coli* isolates from feces of healthy adults bound only to trimannose (Man 3) receptors (16). In addition, type 1 pili are responsible for bacterial invasion and persistence in target cells (17). Moreover, type 1 pili have been implicated in the development of inflammatory and potentially harmful reactions in the host after bacterial infections (18). Type 1 pili are right-handed, 6.9 nm wide pilus rod containing 500-3000 copies of the major structural subunit FimA, and several copies of the minor subunits FimG and FimF (19), and a linear tip fibrillum composed of a highly conserved lectin, the adhesin FimH. FimH is responsible for the bacterial binding to D-mannose moieties on cell-bound and secreted glycoproteins or to non-glycosylated peptide epitopes (20). This allows bacterial adhesion to a wide range of cells, including epithelial and immune cells (21). In addition, FimH can mediate the invasion of uropathogenic *E. coli* into human bladder epithelial cells by triggering host cell signaling cascades. The internalization of *E. coli* by mast cell and macrophage was initiated following the interaction of FimH adhesin with CD48, a glycosylphosphatidylinositol (GPI)-anchored receptor (22, 23).


2.2. Type 3 fimbriae

Type 3 fimbriae are 2 to 4 nm wide and 0.5 to 2 μm long appendages. The fimbriae, as well as type 1 fimbriae, are produced using the chaperone-usher assembly pathway (24, 25, 26). Although type 3 fimbriae are not expressed in *E. coli*, they have been shown to be frequently produced by species of *Enterobacter*, *Proteus*, *Serratia*, *Yersinia*, and by most of the *Klebsiella* isolates associated with human urinary or respiratory tract infections (27). Type 3 fimbriae are morphologically similar to type 1 fimbriae and are characterized by their small diameter and non-channeled structure (28). Type 3 fimbriae are encoded by *mrkABCDF* gene cluster responsible for regulating fimbrial expression (29). The major fimbrial subunit encoding gene *mrkA* is conserved within *Eenterobacteria* (28). Microorganisms expressing type 3 fimbriae demonstrate a mannose resistance (MR) agglutination of erythrocyte suspensions only after the erythrocytes have been pretreated with 0.01% tannic acid and this hemagglutination (HA) occurs in the presence or absence of D-mannose (30) and hence they are usually classified as MR hemagglutinins. Recent investigations have shown that type 3 fimbrial adherence is mediated by the fimbrial minor subunit MrkD, and the adhesion is inhibited by spermidine (31). It has also been reported that the N terminal domain of the minor subunit MrkD adhesin is responsible for receptor binding. The C-terminal region of MrkD possesses sequence motifs that are conserved among several fimbrial adhesins, which are believed to play a role in the folding and assembly of the adhesins (32, 33). MrkB is a periplasmic chaperone and MrkC, an outer membrane usher protein, anchors the fimbriae to the bacterial cell wall. Downstream of *mrkD* gene is *mrkF* gene of which the encoding product has been reported to affect the stability of the intact fimbrial appendage on the bacterial surface (34).

Type 3 fimbriae of *K. pneumoniae* have been shown to influence the

development of biofilms in plastic (35). Growth of *K. pneumoniae* on abiotic surfaces is facilitated, in part, by the major fimbrial subunit MrkA protein, whereas growth on surfaces coated with a human extracellular matrix (HECM) requires the presence of the minor subunit MrkD adhesin (35, 36, 37). In addition, type 3 fimbriae have been suggested to mediate the bacterial attachment to the basolateral surfaces of several types of cells such as tracheal epithelial cells (38), renal tubular cells (7), extracellular matrix proteins (39) and to components of basement membranes of human lung tissue (38). It has also been suggested that type 3 fimbriae facilitate colonization of denuded and damaged epithelial surfaces of debilitated patients in the hospital environment (29). Specifically, type IV and type V collagen may be targets for the attachment (40). However, receptor of type 3 fimbriae on collagen is still unknown.

3. Pilus biogenesis



The mechanism of pilus biogenesis has been mostly characterized for *E. coli* P-pili that was correlated to acute pyelonephritis as well as to first-time cystitis (41). In the system, encoded by *pap* gene cluster, fimbrial subunits are immunoglobulin (Ig)-like form lacking the C-terminal β -strand required to complete the Ig-fold. The subunits form pili through a donor strand exchange reaction, whereby every subunit donates its N-terminal extension to complete the Ig fold of its neighbor, thus forming a noncovalent Ig-like polymer (42). The absence of the C terminal β -strand makes folding of the subunits dependent upon the periplasmic chaperone, which comprises two Ig-like domains (43, 44). Chaperone-subunit interaction facilitates the release of the subunit from the cytoplasmic membrane by its folding directly on the chaperone template. The recognition by chaperone of the conserved hydrophobic carboxyl termini of pilus subunits may trigger the binding of the chaperone to the subunit at the membrane. The chaperone binds to the folded subunit, stabilizing it and capping its

interactive surfaces and thus preventing premature aggregation in the periplasm (45). Each subunit probably exists in a folded conformation in its preassembly complex with chaperone. The preassembly complexes are then targeted to the outer membrane protein usher, which forms a 2-3 nm diameter donut-shaped channel, large enough to allow the passage of pilus subunits (46, 47). It has been shown that the chaperone-adhesin complex has the highest affinity for usher and therefore binds first to it, and that is thought to initiate pilus assembly. An assembly-competent form is maintained throughout pilus assembly process by the formation of a chaperone-adhesin-usher ternary complex (47, 48). The pilus is thought to grow through the usher as a linear fiber upon the bacterial surface (47).

This pilus biogenesis pathway is conserved in a variety of pathogenic bacteria responsible for a wide range of diseases, such as UTIs, diarrhea, pneumonia, plague, and meningitis (49). Therefore, inhibition of the chaperone/subunit complexes by peptidomimetics could be an effective way of controlling UTIs caused by UPEC (50). In fact, it has recently reported that native peptides from FimC chaperone or type 1 pilus proteins were able to block FimC/FimH complexation (51). Investigations have demonstrated that binding to target cells of type 1 fimbriae as well as the *E. coli* P pili is influenced by amino acids which make up the N-terminal regions of the respective adherence molecules (21, 26). The variation of PapG, the adhesin of P fimbriae, also appeared to alter the fimbrial receptor specificity, not only for the type of glycosphingolipids they bind but also for the types of eukaryotic cells to which they attach (52, 53).

4. Specific aims

4.1. To localize the region of MrkD involved in receptor binding.

It has been reported that type 3 fimbrial adhesin is most likely the determinant of

tissue tropism (38, 55). Three allelic variants of the *mrkD* gene of *K. pneumoniae*, a plasmid-encoded MrkD_{1p} and chromosomally occurred MrkD_{1C1} and MrkD_{1C2}, have been reported and mediate binding to various components of the extracellular matrix (54). Our recent investigations have also identified four *mrkD* genotypes, namely *mrkDv1*, *mrkDv2*, *mrkDv3* and *mrkDv4*. Heterologous expression of the fimbriae carrying each of the *mrkD* variants on *E. coli* revealed that the recombinant fimbriae with MrkDv3 on the fibrillum tip has the highest activity in the assay of collagen binding and biofilm formation. Sequence comparison of MrkDv3 with other MrkD variants revealed a varied region from Gly₁₂₀ to Gln₁₄₀ (Fig. 1). In order to determine if the variation affects the fimbrial activity, the recombinant clones carrying different truncated forms of MrkDv3 including MrkDv3_{1-170aa}, MrkDv3_{1-150aa}, and MrkDv3_{1-120aa} were generated and the proteins were purified for competition assays.

4.2. To define the location and functional role of MrkF on type 3 fimbriae

There has been only one study about MrkF, which showed that MrkF affected stability of the fimbriae and hence concluded that MrkF was one of the fimbrial components (56). Sequence analysis showed that MrkF has signal peptides as those of other subunits and a pilin domain as MrkA and MrkD (Fig. 2). We have shown previously that the *E. coli* carrying the plasmid pmrkABCF expressed fimbriae as well as the one carrying the expression plasmid pmrkABCD while *E. coli* carrying pmrkABC were not fimbriation. This suggested that, in addition to MrkD, which has been shown as an initiator in pilus biogenesis (57), MrkF likely plays a role in assembly of the fimbriae. Specifically, the role of MrkF is to be demonstrated using immunomicroscopy, immunoprecipitation and also several activity assays for type 3 fimbriae.

Materials and Methods

1. Strains, plasmids and growth conditions

The bacteria strains, plasmids and primers used in this study are listed in the Tables 1, 2, and 3. The bacteria were propagated at 37°C in Luria Broth (LB) or glycerol-cassamino acid (GCAA) medium with appropriate antibiotics which include ampicillin (100 µg/ml), kanamycin (25 µg/ml) and chloramphenicol (35 µg/ml). The bacterial growth was determined by measuring the optical density at 600 nm (OD₆₀₀).

2. Recombinant DNA technology- MrkD and MrkF clones

The recombinant MrkD clones were constructed by PCR cloning using pMrkDv3 (72) as the template to amplify 984 bp, 549 bp, 477 bp, 360 bp DNA fragments encoding the entire MrkDv3, N-terminal 183 aa (MrkDv3NL), N-terminal 159 aa (MrkDv3N), and N-terminal 120 aa (MrkDv3NS) of MrkDv3 into the expression plasmid pET30a (Novagen) with N-His tag in-framed fusion respectively by *Hind*III and *Xho*I sites. In addition, the signal peptide sequences of all the MrkD recombinant proteins were removed and the resulting constructs were named as dMrkDv3, dMrkDv3NL, dMrkDv3N, dMrkDv3NS.

In order to assist folding of the recombinant MrkD protein, pdMrkB-1-pET was co-transformed with pdMrkDv3-1-pAC into *E. coli* BL21(DE3). The plasmid pdMrkB-1-pET containing 659 bp *mrkB* gene, lacking the signal peptide sequence, was constructed by insertion the fragment amplified from the genome of *K. pneumoniae* liver abscess isolate NTUH-K2044 (71) into the expression vector pET30a by *Nde*I and *Not*I site. The plasmid pdMrkDv3-1-pAC containing *dmrkDv3* gene, lacking the signal peptide sequence was subcloned from pdMrkDv3-YT which was constructed by insertion the PCR fragment of 950 bp into YT&A cloning vector

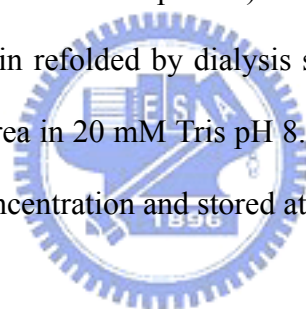
(Yeastern Biotech).

The recombinant plasmid, pmrkABCF, was constructed by insertion of 0.7 kb *mrkF* coding fragment amplified from *K. pneumoniae* NTUH-K2044 into pMrkABC (72) by *ApaI* site. Same approach was employed for construction of the plasmid pmrkABCD, which was cloned by insertion of 1 kb *mrkD* fragment into pMrkABC by *AscI* site and *ApaI* site. The plasmid pmrkABCDF was subcloned by insertion of the 0.7 kb *mrkF* amplicon into pmrkABCD by *ApaI* site.

3. Protein expression and purification

After transformation into *E. coli* BL21(DE3), the recombinant clones that produced MrkD were identified by sodium dodecyl sulfate-polyacrylamide gel electrophoresis (SDS-PAGE). According to the method (76), for large-scale purification of the recombinant MrkD, 100 ml bacteria at 600 nm (A_{600}) of 0.6 were induced with 0.5 mM isopropyl- β -D- thiogalactopyranoside (IPTG) and cultured for an additional 4 h. The pellet was collected by centrifugation and resuspended in 10 ml protein lysis buffer (50 mM Tris-HCl pH 8.0, 1 mM EDTA, 100 mM NaCl). Total cell lysates were sonicated with short burst of 1 sec followed by intervals of 1 sec for cooling and the sonication processing was maintained for 3 min. By ultracentrifugation (13000 rpm, 15 min), the insoluble MrkD protein was remained in pellet. Pellet was washed twice with Wash I buffer (50 mM Tris-HCl pH 8.0, 1 mM EDTA, 100 mM NaCl, 1% TritonX-100) and twice with Wash II buffer (50 mM Tris-HCl pH 8.0, 1 mM EDTA, 100 mM NaCl, 2% sodium deoxycholate). During wash step, pellet must be incubated with Wash II buffer and rocked for 20 min at room temperature before centrifugation. Subsequently, pellet was washed again with the protein lysis buffer. Finally, the insoluble MrkD protein was denatured by 6 M urea in binding buffer (5 mM imidazole, 0.5 M NaCl, 20 mM Tris-HCl pH 7.9). The

recombinant MrkD protein carried an N-terminal polyhistidine tail that efficiently binds to nickel ions and was purified from inclusion bodies of urea-treated cells by affinity chromatography on nickel-nitrilotriacetic acid resin (Novagen, Madison, WI). After washed by sterile water, the column was immersed by charge buffer (50 mM NiSO₄) to the charged resin. To facilitate binding of the protein and resin, the charged resin was immersed in binding buffer with 6 M urea. Then, the denatured recombinant protein was added to column and additional binding buffer with 6 M urea also added. To wash out unbound or only loosely bound proteins, the column was washed with 6 M urea in wash buffer (60 mM imidazole, 0.5 M NaCl, 20 mM Tris-HCl, pH 7.9). Finally, the protein bound to resin were eluted by 6 M urea in elution buffer (1 M imidazole, 0.5 M NaCl, 20 mM Tris-HCl pH 7.9). The urea contained in the solution was diminished and the protein refolded by dialysis stepwise against the buffer with decreasing concentration of urea in 20 mM Tris pH 8.0. The purified protein was then concentrated to an optimal concentration and stored at 4°C.

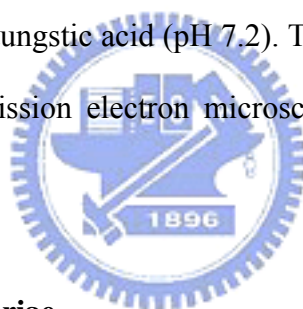


4. Generation of anti-MrkF and anti-MrkD antibody

Five-week-old female BALB/c mice, purchased from National Laboratory Animal Center, received injection in peritoneal cavity with 3-50 µg/150 µl dMrkDv3N on day 1, 11, 15, and 19 respectively. For the first injection, the same volume of Freund's complete adjuvant was used, and Freund's incomplete adjuvant was used for the following times. The dMrkDv3N antiserum was finally obtained by intracardiac puncture. Indirect ELISA (I-ELISA) was performed to test the titer of serum from the tail on day 19 and 23 and the blood serum was harvested from the blood of the mice's heart. Immunization scheme was the same for producing MrkF antibody.

5. Electronic microscopy

As described (27), bacteria from overnight cultures were re-suspended in PBS, and 20 μ l of the suspension was placed on a Formvar carbon-coated glow-discharged grid for 1 min. After placing 3 drops of 2% phosphotungstic acid (pH 7.2) on parafilm, the grid was positioned on this drop for 1 min and the drop was blotted off using filter paper. Finally, after drying the grid, the specimen was ready for examination. For immuno-labeling, the polyclonal antibody in 0.3% BSA in PBS (diluted 1: 50) was applied to the specimen supporting grids and incubated at 4°C overnight. After washed twice with phosphate-buffered saline (PBS), the specimen grid was incubated with the anti-mouse IgG conjugated with 10-nm gold (diluted 1:65) for 60 min at room temperature. After two washing steps with PBS, the specimen-containing grid was stained with 2% phosphotungstic acid (pH 7.2). The grids were examined under a JEOL JEM-2000EXII transmission electron microscope at an operating voltage of 100 kV.



6. Purification of type 3 fimbriae

The fimbriae purification process was carried out with a minor modification of the described method (58). The recombinant *E. coli* JM109[pmrkABCDF] and JM109[pmrkABCD] were cultured for 25 h in 1.5 L LB broth, and the bacteria collected by centrifugation for 30 min (8,000 rpm, 4°C) and suspended in 100 ml phosphate-buffered saline (PBS). The bacterial suspension was heated 3 h at 65°C and then homogenized in blender for 20 min at ambient temperature. The cells were removed by centrifugation (8000 rpm, 20 min) and sodium azide (0.1% w/v) was added to the supernatant. Subsequently, sodium deoxycholate was added to the suspension to a concentration of 0.1% (w/v) and the suspensions were kept at 4°C overnight. After centrifuged for 3 h (20,000 rpm, 4°C), the pellets were suspended

with PBS and a further centrifugation at 13,200 rpm for 5 min. Finally, the type 3 fimbriae-containing supernatant was stored at 4°C.

7. Co-immunoprecipitation

Co-immunoprecipitation was performed according to the procedures described (59). Briefly, 200 µl of the purified fimbriae (100 µg) were incubated with Bovine serum albumin (5 µg/ml), and anti-MrkA antibody (2 µl) and anti MrkF antibody (2 µl) were added respectively to the reactions. After incubation with gentle rocking overnight at 4°C, protein A-Sepharose beads (50 µl) (Amersham) were then added followed by a second incubation for 3 h at 4°C. The protein A-sepharose beads were collected by centrifugation at 6,000 rpm for 3 min, washed three times with 1 ml of 0.1% DOC, and resuspended in 40 µl of protein lysis buffer (50 mM Tris-HCl pH 8.0, 1 mM EDTA, 100 mM NaCl) and 10 µl of 5 x protein sample buffer. Finally, after incubation at 95°C for 10 min, 20 µl of the immunoprecipitate was analyzed by SDS-PAGE and visualized via western blotting hybridization with either anti-MrkA or anti-MrkF antibody.

8. Western blotting analysis

As the method described (48), total cell lysates were resolved by 12.5% sodium dodecyl sulfate-polyacrylamide gel electrophoresis (SDS-PAGE), and the proteins were electrophoretically transferred to polyvinylidene difluoride membranes (ImmobilonTM-P, Millipore). Subsequently, the membranes were blocked with 5% skim milk in 1 x phosphate-buffered saline (PBS) at 4°C for overnight. After washing 3 times with 1 x PBS, the membranes were incubated with a 3000-fold diluted MrkA or MrkF anti-serum at room temperature for 2 h. Followed by incubation with a 10000-fold diluted alkaline phosphatase-conjugated anti-mouse immunoglobulin G at room temperature for 2 h, additional 3 washes were applied and the bound antibodies

were detected by using the chromogenic reagents BCIP (5-bromo-4-chloro-3-indolyl phosphate) and NBT (Nitro blue tetrazolium).

9. Collagen binding assay

Collagen binding assay was carried out as described (39). Briefly, the wells of flat bottom microtiter plates were coated following incubation overnight at 4°C with 0.5 mg/ml of type IV or V collagen diluted in carbonate- bicarbonate buffer, pH 9.6. Each sample was performed triplicate. Prior to incubation with bacteria, nonspecific binding sites were blocked by incubation for 2 h at 22°C with a 2% (w/v) solution of bovine serum albumin in PBS. Subsequently, 100 µl of bacterial suspensions (10^{10} bacteria/ml) prepared in phosphate-buffered saline-Tween 20 (PBS-T) (pH 7.4; 0.5 ml Tween 20 in 1 liter of PBS), was added to the wells. Following incubation for 2 h at 22°C with gentle shaking, unattached bacteria were removed by washing three times in PBS-T. For each well, the adherent bacteria were washed out by 0.1% Triton X-100, diluted in optimal concentration, and plated onto LB agar plates for colony formation.

10. Biofilm formation assay

The ability of bacteria to form biofilm in vitro was detected using the microtiter plate assay with a minor modification of the described method (60). One hundred microliters of overnight grown bacteria diluted 1/100 in LB broth were inoculated into each well of a 96-well microtiter dish and incubated at 37°C for 48 h to allow the formation of biofilm. After thorough by washing the dish with water, 150 µl of crystal violet (1%) was added to each well and the plate was incubated for 30 min at room temperature. The plate was then washed with water, the dye was solubilized in 1% SDS (150 µl/well), and the absorbance at 595 nm was determined. Each biofilm

formation was presented by the average absorbance of three independent experiments.

11. Autoaggregation assay

As described (61), settling profiles were performed on overnight cultures (4 ml) grown in GCAA broth at 37°C. At the beginning, all cultures were shaking vigorously for 20 sec. Samples (10 µl) were taken from the top of the culture at regular time intervals and were spread on microscope slide. After dried by heat, the samples were stained with 1% crystal violet and roasted again. Then, the samples were observed under light microscopy with 100 x object lens.



Results

1. Overexpression and purification of MrkD and MrkB recombinant proteins

Our previous studies have shown that sequence variation of MrkD influenced the expression of type 3 fimbriae, which include changes in the activities of collagen binding and biofilm formation, and morphology of the fimbriae. In addition, the recombinant *E. coli* displaying with type 3 fimbriae of *mrkDv3* was found to have the highest level of either collagen binding or biofilm formation activity. As shown in Fig. 1, sequence comparison of MrkDv3 with the other MrkD variants, MrkDv1, MrkDv2, MrkDv4 and MrkD_{ntub}, revealed a variable region from Gly₁₂₀ to Gln₁₄₀. It is interestingly to note that RGD residues which are active modulators of cell adhesion are contained in the region. As shown in Fig. 2, a signal peptide sequence in MrkF was observed and a conserved pilin domain of MrkA (34) was found also to be contained in MrkF suggesting that MrkF is a component of type 3 fimbriae.

In order to determine the role of the variation, MrkDv3, MrkDv3NL, MrkDv3N, and MrkDv3NS containing expression plasmids were generated. As shown in Fig. 3, MrkDv3N contained the N-terminal domain of MrkDv3 from residues 1 to 159, and MrkDv3NS contained residues 1 to 120, lacking the variable region Gly₁₂₀ to Gln₁₄₀, while MrkDv3NL contained the region from residues 1 to 183. Total cellular proteins from each of the recombinant bacteria containing the plasmids expressing respectively the proteins, MrkDv3, MrkDv3NL, MrkDv3N, and MrkDv3NS, were collected and analyzed by SDS-PAGE. As shown in Fig. 4A and 4B, the recombinant protein MrkDv3 and MrkDv3NL induced by IPTG, with the final concentration of either 0.1 µg/ml or 0.5 µg/ml, could be observed with the predicted size of 37 kDa (MrkDv3) and 27.9 kDa (MrkDv3NL). However, the proteins formed inclusion bodies. In order to improve the solubility, several methods such as 25°C induction

(lanes 8-10 in Fig. 4A and 4B) and lower concentration of IPTG (0.1 $\mu\text{g/ml}$, lanes 2-7 in Fig. 4A and 4B) were tried but failed. Similarly, as shown in Fig 4C and 4D, the IPTG inducible proteins MrkDv3N and MrkDv3NS with the predicted size 25 kDa and 23 kDa, respectively, remained insoluble form.

In case that not enough chaperone proteins are present for properly folding of the overexpressed proteins, the recombinant plasmid pdMrkB-1-pET, containing the MrkB chaperone protein encoding gene, was generated and co-expressed with pdMrkDv3-1-pAC in the recombinant *E. coli*. In addition, the signal peptides of MrkB and MrkD proteins were both removed to avoid from aggregation in the periplasm. Whatsoever, even the recombinant chaperone proteins appeared to be insoluble (data not shown). Finally, the recombinant protein dMrkDv3N were purified by denaturalization using 6 M urea and were refolded by dialysis against the buffer of 20 mM Tris-HCl containing 20% glycerol. Nevertheless, most of the proteins remained aggregated and only a small amount of protein obtained with a concentration of 54 $\mu\text{g/ml}$.

2. Analysis of the purified dMrkDv3N in competition assay.

The purified dMrkDv3N, containing the N-terminal 159 amino acids was subsequently added as a competitor in the collagen IV binding assay. As shown in Fig. 5, the purified dMrkDv3N proteins added with either 5.4 μg or 8.1 μg respectively appeared to reduce the binding of *E. coli* JM109[pMrkABCDv3F] to the type IV collagen. The inhibition was enhanced with the increasing of the recombinant protein dMrkDv3N indicating that the N-terminal 159 amino acids containing MrkDv3 is able to compete for the type IV collagen binding activity of the *E. coli* JM109[pMrkABCDv3F].

3. MrkF is a component of type 3 fimbriae

As shown in Fig. 6A, a protein band corresponding to the predicted size of MrkA could be observed. After the gel hybridization with anti-MrkF antiserum, a protein band appropriate for 22 kDa, which is the predicted size for MrkF, was detected indicating the specificity of the raised antibody (Fig. 6B).

In order to know whether MrkF is a component of type 3 fimbriae, type 3 fimbriae were purified from JM109[pmrkABCDF] and analyzed by SDS-PAGE and further detected with anti-MrkF and anti-MrkA antibodies. As shown in Fig. 7A and B, the MrkA corresponding band with approximately 23 kDa could be observed in the purified fimbriae from JM109[pmrkABCDF] and JM109[pmrkABCD]. While analyze with anti-MrkF antibody, the detected band of approximately 22 kDa could only be found in the purified fimbriae from JM109[pmrkABCDF] (Fig. 7C). According to the reported fimbrial organization of several well-known fimbriae, the filament is constructed by subunit association (77). As a component of type 3 fimbriae, MrkF must interact with MrkA in some way to form a fimbria. Using anti-MrkA antibody or anti-MrkF antibody appeared to be able to pull down both MrkA and MrkF from the purified fimbriae of JM109[pmrkABCDF] and JM109 [pmrkABCF] as detected by either anti-MrkA antibody (Fig. 8A) or anti-MrkF antibody (Fig. 8B). In contrast, the pull down lysates from the purified fimbriae of JM109 [pmrkABCD] could only be detected by anti-MrkA antibody.

Subsequently, localization of MrkF on type 3 fimbriae was demonstrated by immuno-electron microscopy (immuno-EM). As shown in Fig. 9, the pili labeled in situ with gold-tagged anti-mouse IgG antibodies against the anti-MrkF antibody revealed the signals at the middle part of the filament suggesting that type 3 fimbriae is consisting of stretches of MrkA interrupted by MrkF at regular intervals.

4. MrkF influences the fimbriation of the recombinant *E. coli*

Although lacking the *mrkD* adhesion gene, a few fimbriae could be observed on the surface of the recombinant *E. coli* HB101[pmrkABCF] (Fig. 10) suggesting that MrkF is an initiator for the assembly of the fimbriae. However, in comparing with that of HB101[pmrkABCD], the limited number of fimbriae on the surface of HB101 [pmrkABCF] also suggested a minor role of MrkF in initiation of the fimbriation. As shown in Fig. 10, the recombinant *E. coli* HB101[pmrkABCDF] exerted more and shorter fimbriae than that of HB101[pmrkABCD] indicating a more efficient fimbriation but a tighter control for the length of the filament. Nevertheless, after being heated at 55°C for 10 min, an obvious falling off of the MrkF-lacking-fimbriae from the bacterial surface supported the role of MrkF as a controller for the stability of type 3 fimbriae as proposed (34)

5. Assessment of the activity of the recombinant type 3 fimbriae

Type 3 fimbriae had been shown to bind specifically to type IV and type V collagen (62). The collagen binding activity of the recombinant *E. coli* JM109[pmrkABCDF], JM109[pmrkABCD] and JM109[pGEMT] were hence compared. The recovered bacteria JM109[pmrkABCDF] were more than JM109[pmrkABCD] in either collagen IV binding assay (Fig. 11A) or collagen V binding assay (Fig. 11B), suggesting that lacking of MrkF causes the lower binding activity to collagen.

Biofilm formation activity of type 3 fimbriae has been demonstrated to be mediated by MrkA or MrkD at different conditions (36, 63). As shown in Fig. 12, the recombinant *E. coli* JM109[pmrkABCDF] appeared to have higher biofilm formation activity than JM109[pmrkABCD] implying that MrkF plays a role in biofilm formation. In addition, the activity of biofilm formation was comparable with

Pseudomonas aeruginosa PAO1, a strong biofilm formation strain, indicated that the recombinant fimbriae produced by *E. coli* JM109[pmrkABCDF] could help efficiently for the biofilm formation. It has previously been demonstrated that the MrkD adhesin of type 3 fimbriae was not required for an efficient biofilm formation on abiotic plastic surface (35). Notably, the *E. coli* JM109[pmrkABCF] which expressed few fimbriae with no MrkD appeared to lose the ability to form biofilm (Fig. 12).

Autoaggregation, which is mediated by bacteria surface self-recognizing adhesins or autoaggregative fimbriae, is a phenomenon thought to contribute to colonization of mammalian hosts by pathogenic bacteria (64, 65, 66, 67). The recombinant *E. coli* JM109[pmrkABCDF] appeared to show conspicuous autoaggregation after overnight cultured in GCAA medium (Fig. 13). In contrast, no autoaggregative appearance could be observed in JM109[pmrkABCD]. This suggested a functional role of MrkF in autoaggregation. To investigate the possibility, *mrkF* gene was introduced respectively into the non-autoaggregative strains, JM109[pmrkABCDv1] and JM109[pmrkABCDv2]. As predicted, introduction of the MrkF encoding gene conferred the bacteria JM109[pmrkABCDv1F] and JM109[pmrkABCDv2F] an autoaggregative phenotype (Fig. 13). In addition, the autoaggregative phenomenon of JM109 [pmrkABCDv3] and JM109 [pmrkABCDv4] could be enhanced after introducing the *mrkF* gene in the bacteria.

Discussions

Fimbriae are important appendages for bacteria to infect host. The adherence to host epithelial of fimbriae influence the host range and tissue tropism of bacteria. Many features of famous pili such as type 1 pilus, P pilus, in uropathogenic *E. coli* were well studied, including adherent receptor, structural components, organization, and their function. However, investigation of type 3 fimbriae which is universal expressed in *Enterobacteriaceae* is still not enough. For example, the assembly model, adhesin structure, and fimbrial organization are poorly understood.

1. Improvement of the solubility of the recombinant protein

In many cases, the insolubility of the recombinant proteins prevent further assays. In this study, several strategies have been tried but failed. Nevertheless, we intend to solve the problem in the future by construction of the recombinant plasmids for optimal expression in AD494 (DE3) or BL21*trxB* (DE3), which is thioredoxin reductase-deficient strain often used to maximize soluble protein expression (78). An alternative approach is to fuse the protein with a solubility-enhancing tag such as the Trx●TagTM, GST●TagTM, or Nus●TagTM sequences (68).

2. Localization of MrkF

So far, there is only one report to suggest the role of MrkF in stabilizing the structure of type 3 fimbriae (34). While analysis of MrkF sequence, a typical signal peptide may found and the sequence alignment with MrkA showed a conserved pilin domain (Fig. 2), implying that MrkF is also a component of type 3 fimbriae. As shown in Fig. 8, co-immunoprecipitation assay demonstrated an

interaction of MrkA and MrkF which supports further the association of MrkF with MrkA on the fimbriae. Moreover, TEM of immuno-gold labeled fimbriae showed that the labeled MrkF appeared to be inserted to the fimbrial shaft at regular intervals. During the assembly of a pilus, the order of subunit on fimbriae is decided by the affinity between subunit-chaperone complexes and usher (75). As shown in the Fig. 9, many MrkA proteins on the fimbriae appeared to be interrupted by a few MrkF suggesting that MrkA-chaperone complexes have higher affinity to usher than the MrkF-chaperone complexes.

3. Functional role of MrkF

The TEM analysis indicated that all the recombinant *E. coli* were fimbriated except HB101[pmrkABC]. The fact that adhesin is an initiator for the assembly of fimbriae has been reported (46, 69). Interestingly, the bacteria HB101[pmrkABCF], lacking the MrkD adhesin as an initiator, appeared to be fimbriated (Fig. 10) suggesting a role of MrkF in initiating the fimbriation. Whatsoever, the bacteria HB101[pmrkABCDF] exhibiting more fimbriae on the surface than HB101[pmrkABCD] supported the role of MrkF in controlling the stability of fimbriae.

In order to colonize surfaces, most bacteria grow as organized biofilm communities (70). Adherence to non-biological surfaces constitutes the first step in biofilm development (13). The type 3 fimbrial major subunit MrkA has been reported to facilitate biofilm formation on abiotic surface (13). The bacteria JM109[pmrkABCDF] having higher biofilm formation activity than JM109[pmrkABCD] could be contributed to the increasing amount of type 3 fimbriae presented on the bacteria surface. On the other hand, the lacking of MrkF in JM109[pmrkABCD] could result in lower level of fimbriation thereby less

MrkA was available to help for biofilm formation.

The attachment of bacteria to a surface often results in the proliferation into complex microcolony structure. A number of factors including antigen 43 (Ag43) (73), curli (74) and type 1 fimbriae (60) have been implicated in microcolony formation and autoaggregation in *E. coli*. In particular, type 1 fimbriae have been shown to confer bacterial autoaggregation and enhance biofilm formation on abiotic surfaces. In *K. pneumoniae*, similar to type 1 fimbriae, type 3 fimbriae appeared to mediate the biofilm formation (13). Aggregation and microcolony formation often prelude to biofilm formation and hence the apparent autoaggregation of the recombinant *E. coli* JM109[pmrkABCDF] led to a high level of biofilm formation activity. As shown in Fig. 13, the recombinant *E. coli* JM109[ABCDF], but not JM109[mrkABCD], appeared to autoaggregate in GCAA medium. Moreover, the autoaggregative phenomenon of the recombinant *E. coli* could be induced by transforming the bacteria with the plasmid carrying a *mrkF* gene, suggesting a role of MrkF in autoaggregative phenotype. It is likely that lacking of MrkF alters the structure of the 3 fimbriae and hence the decreasing activity of autoaggregation. Overall, this study indicated that MrkF is a component of type 3 fimbriae and a role of MrkF in initiating the fimbriation was also suggested.

References

1. Chen, K.Y., Hsueh, P.R., Liaw, Y.S., Yang, P.C. and Luh, K.T., 2000. A 10-year experience with bacteriology of acute thoracic empyema: emphasis on *Klebsiella pneumoniae* in patients with diabetes mellitus. *Chest*. 117, 1685-1689.
2. Williams, P., and Tomas, J.M., 1990. The pathogenicity of *Klebsiella pneumoniae*. *Rev. Med. Microbiol.* 1, 196-204.
3. Mayhall, C.G., Lamb, V.A., Bitar, C.M., Miller, K.B., Furse, E.Y., Kirkpatrick, B.V., Markowitz, S.M., Veazey, J.M.Jr. and Marcrina, F.L., 1980. Nosocomial *Klebsiella* infection in a neonatal unit: identification of risk factors for gastrointestinal colonization. *Infect. Control*. 1, 239-246.
4. Lee, P.Y., Chang, W.N., Lu, C.H., Lin, M.W., Cheng, B.C., Chien, C.C., Chang, C.J. and Chang, H.W., 2003. Clinical features and *in vitro* antimicrobial susceptibilities of community-acquired *Klebsiella pneumoniae* meningitis in Taiwan. *J. Antimicrob. Chemother.* 51, 957-962.
5. Tarkkanen, A.M., Allen, B.L., Williams, P.H., Kauppi, M., Haahtela, K., Siitonen, A., Orskov, I., Orskov, F., Clegg, S. and Korhonen, T.K., 1992. Fimbriation, capsulation, and iron-scavenging systems of *Klebsiella* strains associated with human urinary tract infection. *Infect. Immun.* 60, 1187-1192.
6. Sauer, F.G., Barnhart, M., Choudhury, D., Knight, S.D., Waksman, G. and Hultgren, S.J., 2000. Chaperon-assisted pilus assembly and bacterial attachment. *Curr. Opin. Struct. Biol.* 10, 548-556.
7. Tarkkanen, A.M., Virkola, R., Clegg, S. and Korhonen, T.K., 1997. Binding of the type 3 fimbriae of *Klebsiella pneumoniae* to human endothelial and urinary bladder cells. *Infect. Immun.* 65, 1546–1549.
8. Di Martino, P., Livrelli, V., Sirot, D., Joly, B. and Darfeuille-Michaud, A., 1996. A new fimbrial antigen harbored by CAZ-5/SHV-4-producing *Klebsiella pneumoniae* strains involved in nosocomial infections. *Infect. Immun.* 64, 2266-2273.
9. Darfeuille-Michaud, A., Jallat, C., Aubel, D., Sirot, D., Rich, C., Sirot, J. and Joly, B., 1992. R-plasmid-encoded adhesive factor in *Klebsiella pneumoniae* strains responsible for human nosocomial infections. *Infect. Immun.* 60:44-55.
10. Zhou, G., Mo, W.J., Sebbel, P., Min, G., Neubert, T.A., Glockshuber, R., Wu, X.R., Sun, T.T. and Kong, X.P., 2001. Uroplakin Ia is the urothelial receptor for uropathogenic *Escherichia coli*: evidence from *in vitro* FimH binding. *J. Cell Sci.* 114, 4095-4103.
11. Sharon, N., 1987. Bacterial lectins, cell–cell recognition and infectious disease.

FEBS Lett. 217, 145-157.

12. Snyder, J.A., Haugen, B.J., Lockett, C.V., Maroncle, N., Hagan, E.C., Johnson, D.E., Welch, R.A. and Mobley, H.L., 2005. Coordinate expression of fimbriae in uropathogenic *Escherichia coli*. *Infect Immun.* 73, 7588-7596.
13. Di-Martino, P., Cafferini, N., Joly, B. and Darfeuille-Michaud, A., 2003. *Klebsiella pneumoniae* type 3 pili facilitate adherence and biofilm formation on abiotic surfaces. *Res. Microbiol.* 154, 9-16.
14. Klemm, P. and Krogfelt, K.A., 1994. Type 1 fimbriae of *Escherichia coli*, pp. 9–26. In *Fimbriae, Adhesion, Genetics, Biogenesis and Vaccines*. Klemm, P. (ed.). Boca Raton, FL: CRC Press.
15. Buchanan, K., Falkow, S., Hull, R.A. and Hull, S.I., 1985. Frequency among Enterobacteriaceae of the DNA sequences encoding type 1 pili. *J. Bacteriol.* 162, 799-803.
16. Firon, N., Ashkenazi, S., Mirelman, D., Ofek, I. and Sharon, N., 1987. Aromatic alpha-glycosides of mannose are powerful inhibitors of the adherence of type 1 fimbriated *Escherichia coli* to yeast and intestinal epithelial cells. *Infect. Immun.* 55, 472-476.
17. Martinez, J.J., Mulvey, M.A., Schilling, J.D., Pinkner, J.S. and Hultgren, S.J., 2000. Type 1 pilus-mediated bacterial invasion of bladder epithelial cells. *EMBO J.* 19, 2803-2812.
18. Malaviya, R., Ross, E., Jakschik, B.A. and Abraham, S.N., 1994. Mast cell degranulation induced by type 1 fimbriated *Escherichia coli* in mice. *J. Clin. Invest.* 93, 1645-1653.
19. Hahn, E., Wild, P., Hermanns, U., Sebbel, P., Glockshuber, R., Haner, M., Taschner, N., Burkhard, P., Aebi, U. and Muller, S.A., 2002. Exploring the 3D molecular architecture of *Escherichia coli* type 1 pili. *J. Mol. Biol.* 323, 845-857.
20. Sokurenko, E.V., Courtney, H.S., Ohman, D.E., Klemm, P. and Hasty, D.L., 1994. FimH family of type 1 fimbrial adhesins: functional heterogeneity due to minor sequence variations among fimH genes. *J. Bacteriol.* 176, 748-755.
21. Sokurenko, E.V., Courtney, H.S., Ohman, D.E., Klemm, P. and Hasty, D.L., 1994. FimH family of type 1 fimbrial adhesins: functional heterogeneity due to minor sequence variations among fimH genes. *J. Bacteriol.* 176, 748-755.
22. Baorto, D.M., Gao, Z., Malaviya, R., Dustin, M.L., Van-der-Merwe, A., Lublin, D.M., Abraham, S.N., 1997. Survival of FimH-expressing enterobacteria in macrophages relies on glycolipid traffic. *Nature* 389, 636–639.
23. Shin, J.S., Gao, Z. and Abraham, S.N., 2000. Involvement of cellular caveolae

- in bacterial entry into mast cells. *Science* 289:785–788.
24. Klemm, P., 1992. FimC, a chaperone-like periplasmic protein of *Escherichia coli* involved in biogenesis of type 1 fimbriae. *Res. Microbiol.* 143, 831–838.
 25. Klemm, P. and Christiansen, G., 1990. The fimD gene required for cell surface localization of *Escherichia coli* type 1 fimbriae. *Mol. Gen. Genet.* 220, 334–338.
 26. Hultgren, S.J. and Normark, S., 1991. Chaperone-assisted assembly and molecular architecture of adhesive pili. *Annu. Rev. Microbiol.* 45, 383–415.
 27. Hornick, D.B., Thommandru, J., Smits, W. and Clegg, S., 1995. Adherence properties of an *mrkD*-negative mutant of *Klebsiella pneumoniae*. *Infect. Immun.* 63, 2026-2032.
 28. Old, D.C. and Adegbola, R.A., 1985. Antigenic relationships among type 3 fimbriae of the enterobacteriaceae revealed by immunoelectron microscopy. *J. Med. Microbiol.* 20, 113-121.
 29. Clegg, S., Korhonen, K.T., Hornick, B.D. and Tarkkanen, A.M., 1994. Type 3 fimbriae of the Enterobacteriaceae, pp. 97–104. In K. P. Klemm (ed.), *Fimbriae: adhesion, genetics, biogenesis, and vaccines*. CRC Press, Boca Raton, Fla.
 30. Duguid, J.P. and Old, D.C., 1980. Adhesive properties of Enterobacteriaceae, pp.185-217. In E. H. Beachey (ed.), *Bacterial adherence*. Chapman and Hall, London.
 31. Kunin, C.M., 1987. *Detection, prevention, and management of urinary tract infections*. Lea & Febiger, Philadelphia, Pa.
 32. Hultgren, S.J., Lindberg, F., Magnusson, G., Kihlberg, J., Tennent, J.M. and Normark, S., 1989. The PapG adhesin of uropathogenic *Escherichia coli* contains separate regions for receptor binding and for the incorporation into the pilus. *Proc. Natl. Acad. Sci. U.S.A.* 86, 4357-4361.
 33. Girardeau, J.P. and Bertin, Y., 1995. Pilins of fimbrial adhesins of different member species of Enterobacteriaceae are structurally similar to the Cterminal half of adhesin proteins. *FEBS Lett.* 357, 103–108.
 34. Allen, B.L., Gerlach, G.F. and Clegg, S., 1991. Nucleotide sequence and functions of mrk determinants necessary for expression of type 3 fimbriae in *Klebsiella pneumoniae*. *J. Bacteriol.* 173, 916-920.
 35. Langstraat, J., Bohse, M. and Clegg, S., 2001. The type 3 fimbrial shaft (MrkA) of *Klebsiella pneumoniae*, but not the fimbrial adhesin (MrkD), facilitates biofilm formation. *Infect Immun* 69, 5805-5812.
 36. Jagnow, J. and Clegg, S., 2003. *Klebsiella pneumoniae* MrkD-mediated biofilm formation on extracellular matrix- and collagen-coated surfaces.

- Microbiology. 149, 2397-2405.
37. Jagnow, J. and Clegg, S., 2003. *Klebsiella pneumoniae* MrkD-mediated biofilm formation on extracellular matrix- and collagen-coated surfaces. *Microbiology*. 149, 2397-2405.
 38. Hornick, D.B., Allen, B.L., Horn, M.A., Clegg, S., 1992. Adherence to respiratory epithelia by recombinant *Escherichia coli* expressing *Klebsiella pneumoniae* type 3 fimbrial gene products. *Infect Immun*. 60:1577-88.
 39. Sebghati, T.A., Korhonen, T.K., Hornick, D.B. and Clegg, S., 1998. Characterization of the type 3 fimbrial adhesins of *Klebsiella* strains. *Infect. Immun*. 66, 2887-2894.
 40. Sebghati, T.A., Korhonen, T.K., Hornick, D.B. and Clegg, S., 1998. Characterization of the type 3 fimbrial adhesins of *Klebsiella* strains. *Infect Immun*. 66, 2887-2894.
 41. Johnson, J.R., Johnson, C.E. and Maslow, J.N., 1999. Clinical and bacteriologic correlates of the papG alleles among *Escherichia coli* strains from children with acute cystitis. *Pediatr. Infect. Dis. J.* 18, 446-451.
 42. Sauer, F.G., Pinkner, J.S., Waksman, G. and Hultgren, S.J., 2002. Chaperone priming of pilus subunits facilitates a topological transition that drives fiber formation. *Cel*. 111, 543-551.
 43. Pellicchia, M., Guntert, P., Glockshuber, R. and Wuthrich, K., 1998. NMR solution structure of the periplasmic chaperone FimC. *Nat. Struct. Biol.* 5, 885-890.
 44. Holmgren, A. and Branden, C.I., 1989. Crystal-structure of chaperone protein PapD reveals an immunoglobulin fold. *Nature*. 342, 248-251.
 45. Soto, G.E., Dodson, K.W., Ogg, D., Liu, C., Heuser, J., Knight, S., Kihlberg, J., Jones, C.H. and Hultgren, S.J., 1998 Periplasmic chaperone recognition motif of subunits mediates quaternary interactions in the pilus. *EMBO J.* 17, 6155-6167
 46. Dodson, K.W., Jacob-Dubuisson, F., Striker, R.T. and Hultgren, S.J., 1993 Outer membrane PapC molecular usher discriminately recognizes periplasmic chaperone]pilus subunit complexes. *Proc. Natl. Acad. Sci. USA* 90, 3670-3674.
 47. Thanassi, D.G., Saulino, E.T., Lombardo, M.J., Roth, R., Heuser, J. and Hultgren, S.J., 1998 The PapC usher forms an oligomeric channel: implications for pilus biogenesis across the outer membrane. *Proc. Natl. Acad. Sci. USA*. 95, 3146-3151.
 48. Saulino, E.T., Thanassi, D.G., Pinkner, J.S. and Hultgren, S.J., 1998. Ramification of kinetic partitioning on usher-mediated pilus biogenesis.

EMBO J. 17, 2177-2185.

49. Hultgren, S.J., Abraham, S., Caparon, M., Falk, P., Stgeme, J. W. and Normark, S., 1993. Pilus and nonpilus bacterial adhesins - Assembly and function in cell recognition. *Cell*. 73, 887- 901.
50. Stephens, C. and Shapiro, L., 1997. Bacterial protein secretion - a target for new antibiotics. *Chem. Biol.* 4, 637-641.
51. Larsson, A., Barnhart, M., Stenstroöm, T., Pinkner, J.S., Hultgren, S.J., Almqvist, F., Kihlberg, J., Manuscript in preparation.
52. Stromberg, N. and Karlsson, K.A., 1990. Characterization of the binding of propionibacterium granulosum to glycosphingolipids adsorbed on surfaces. An apparent recognition of lactose which is dependent on the ceramide structure. *J. Biol. Chem.* 265, 11244-11250.
53. Stromberg, N., Nyholm, P.G., Pascher, I. and Normark, S., 1991. Saccharide orientation at the cell surface affects glycolipid receptor function. *Proc. Natl. Acad. Sci. USA*. 88, 9340-9344.
54. Sebghati, T.A., Korhonen, T.K., Hornick, D.B. and Clegg, S., 1998. Characterization of the type 3 fimbrial adhesins of *Klebsiella* strains. *Infect Immun.* 66, 2887-2894.
55. Schurtz, T.A., Hornick, D.B., Korhonen, T.K. and Clegg, S., 1994. The type 3 fimbrial adhesin gene (*mrkD*) is not conserved among all fimbriate strains. *Infect. Immun.* 62, 4186-4191.
56. Gerlach, G.F., Clegg, S. and Allen, B.L., 1989. Identification and characterization of the genes encoding the type 3 and type 1 fimbrial adhesins of *Klebsiella pneumoniae*. *J. Bacteriol.* 171, 1262-1270.
57. Barnhart, M.M., Sauer, F.G., Pinkner, J.S. and Hultgren, S.J., 2003. Chaperone-subunit-usher interactions required for donor strand exchange during bacterial pilus assembly. *J. Bacteriol.* 185, 2723-2730.
58. Sakellaris, H., Balding, D.P. and Scott, J.R., 1996. Assembly proteins of CS1 pili of enterotoxigenic *Escherichia coli*. *Mol. Microbiol.* 21, 529-541.
59. Jakubowski, S.J., Krishnamoorthy, V. and Christie, P.J., 2003. *Agrobacterium tumefaciens* VirB6 Protein Participates in Formation of VirB7 and VirB9 Complexes Required for Type IV Secretion. *J. Bacteriol.* 185, 2867-2878.
60. Schembri, M.A. and Klemm, P., 2001. Biofilm formation in a hydrodynamic environment by novel fimH variants and ramifications for virulence. *Infect Immun.* 69, 1322-1328.
61. Schembri, M.A., Christiansen, G. and Klemm, P., 2001. FimH-mediated autoaggregation of *Escherichia coli*. *Mol. Microbiol.* 41, 1419-1430.
62. Tarkkanen, A.M., Allen, B.L., Westerlund, B., Holthofer, H., Kuusela, P.,

- Risteli, L., Clegg, S. and Korhonen, T.K., 1990. Type V collagen as the target for type-3 fimbriae, enterobacterial adherence organelles. *Mol. Microbiol.* 4, 1353-1361.
63. Baddour, L.M., Christensen, G.D., Simpson, W.A. and Beachey, E.H., 1989. In *Principles and Practice of Infectious Disease*, eds. Mandell, G. L., Dangles, R.G. and Bennet, J.E. (Churchill Livingstone, New York), 2, 9-25.
64. Hasman, H., Chakraborty, T. and Klemm, P., 1999. Antigen-43-mediated autoaggregation of *Escherichia coli* is blocked by fimbriation. *J. Bacteriol.* 181, 4834-4841.
65. Kjaergaard, K., Schembri, M.A., Hasman, H. and Klemm, P., 2000. Antigen 43 from *Escherichia coli* induces inter- and intraspecies cell aggregation and changes in colony morphology of *Pseudomonas fluorescens*. *J. Bacteriol.* 182, 4789-4796.
66. Haussler, S., Ziegler, I., Lottel, A., von-Gotz, F., Rohde, M., Wehmhohner, D., Saravanamuthu, S., Tummler, B. and Steinmetz, I., 2003. Highly adherent small-colony variants of *Pseudomonas aeruginosa* in cystic fibrosis lung infection. *J. Med. Microbiol.* 52, 295-301.
67. Collinson, S.K., Doig, P.C., Doran, J.L., Clouthier, S., Trust, T.J. and Kay, W.W., 1993. Thin, aggregative fimbriae mediate binding of *Salmonella enteritidis* to fibronectin. *J. Bacteriol.* 175, 12-18.
68. Davis, G.D., Elisee, C., Newham, D.M. and Harrison, R.G., 1999. New fusion protein systems designed to give soluble expression in *Escherichia coli*. *Biotechnol. Bioeng.* 65, 382-388.
69. Saulino, E.T., Thanassi, D.G., Pinkner, J. and Hultgren, S.J., 1998. Ramifications of kinetic partitioning on usher-mediated pilus biogenesis. *EMBO J.* 17, 2177-2185.
70. Stickler D., 1999. Biofilms, *Curr. Opin. Microbiol.* 2, 270-275.
71. Ma, L.C., Fang, C.T., Lee, C.Z., Shun, C.T. and Wang, J.T., 2005. Genomic heterogeneity in *Klebsiella pneumoniae* strains is associated with primary pyogenic liver abscess and metastatic infection. *J. Infect. Dis.* 192, 117-128.
72. Chen, M.C., 2003. Characterization of the Type 3 Fimbrial Adhesins of *Klebsiella pneumoniae*. Master thesis, Chiao Tung University Press.
73. Hasman, H., Schembri, M.A. and Klemm, P., 2000. Antigen 43 and type 1 fimbriae determine colony morphology of *Escherichia coli* K-12. *J. Bacteriol.* 182, 1089-1095.
74. Prigent-Combaret, C., Brombacher, E., Vidal, O., Ambert, A., Lejeune, P., Landini, P. and Dorel, C., 2001. Complex regulatory network controls initial adhesion and biofilm formation in *Escherichia coli* via regulation of the *csgD*

- gene. *J. Bacteriol.* 183, 7213–7223.
75. Thanassi, D.G., Stathopoulos, C., Dodson, K., Geiger, D. and Hultgren, S.J., 2002. Bacterial outer membrane ushers contain distinct targeting and assembly domains for pilus biogenesis. *J. Bacteriol.* 184, 6260-6269.
 76. Nishiyama, M., Vetsch M., Puorger C., Jelesarov I. and Glockshuber R., 2003. Identification and characterization of the chaperone-subunit complex-binding domain from the type 1 pilus assembly platform FimD. *J Mol Biol.* 330, 513-525.
 77. Sauer, F.G., Knight S.D., Waksman, G.J. and Hultgren S.J., 2000. PapD-like chaperones and pilus biogenesis. *Semin Cell Dev Biol.* 11, 27-34.
 78. Derman, A.I., Prinz, W.A., Belin, D. and Beckwith, J., 1993. Mutations that allow disulfide bond formation in the cytoplasm of *Escherichia coli*. *Science.* 262, 1744-1747.



Table 1. Bacteria strains used in this study

strains	Genotypes or relevant properties	Reference or source
<i>Escherichia coli</i>		
NovaBlue(DE3)	<i>endA1 hsdR17</i> (rk ₁₂ ⁻ mk ₁₂ ⁺) <i>supE44</i> <i>thi-1 recA1 gyrA96 relA1 lac</i> [F' <i>pro AB</i> <i>lac^gZΔM15::Tn10</i>](DE3);Tet ^r	Novagen
BL21(DE3)	<i>F ompT hsdS_B</i> (rb ⁻ mb ⁻) <i>gal dcm</i> (DE3)	Laboratory stock
JM109	<i>RecA1 supE44 endA1 hsdR17 gyrA96</i> <i>RelA1 thiΔ</i> (<i>lac⁻proAB</i>)	Laboratory stock
HB101	<i>F⁻ thi-1 hsdS20</i> (rb ⁻ mb ⁻) <i>supE44</i> <i>recA13 ara-14 leuB6 proA2 lacY1</i> <i>galK2, rpsL20</i> (str ^r) <i>xyl-5 ml-1</i>	Laboratory stock
<i>Klebsiella pneumoniae</i>		
<i>k. p</i> NTUH k-2044	Clinical isolate	71
VHm5	Clinical isolate	Veteran General Hospital
<i>Pseudomonas aeruginosa</i>		
PAO1		Laboratory stock



Table 2. Plasmids used and constructed in this study

Plasmids	Relevant characteristic	Reference or source
pGEMT	Cloning vector ; Ap ^r	Promega
yT&A	Cloning vector ; Ap ^r	Yeastern Biotech
pET30a-c	Expression vector ; Kan ^r	Novagen
pACYCDuet-1	Expression vector ; Cm ^r	Novagen
pMrkDv3	1 kb fragment amplified using VHM5 chromosome as template and primer pairs, MZ007 and MZ008, and cloned into pET30a by <i>Hind</i> III and <i>Xho</i> I site, Kan ^r	72
pdMrkDv3-YT	950 bp fragment amplified using pMrkDv3 as template and primer pairs, phw19 and phw12, and cloned into YT&A, Ap ^r	This study
pdMrkDv3	<i>dmrkDv3</i> fragment digested from pdMrkDv3-YT and cloned into pET30a by <i>Sac</i> I and <i>Xho</i> I site, Kan ^r	This study
pdMrkDv3-1-pAC	<i>dmrkDv3</i> fragment digested from pdMrkDv3-YT using <i>Sal</i> I and <i>Hind</i> III site and cloned into pACYCDuet-1 expression vector, Cm ^r	This study
pMrkDv3NL	549 bp fragment amplified using pMrkDv3 as template and primer pairs, MZ007 and phw12, and cloned into pET30a by <i>Hind</i> III and <i>Xho</i> I site, Kan ^r	This study
pdMrkDv3NL	500 bp fragment amplified using pMrkDv3 as template and primer pairs, phw19 and phw12, and cloned into pET30a by <i>Sac</i> I and <i>Xho</i> I site, Kan ^r	This study
pMrkDv3N	477 bp fragment amplified using pMrkDv3 as template and primer pairs, MZ007 and phw07, and cloned into pET30a by <i>Hind</i> III and <i>Xho</i> I site, Kan ^r	This study
pdMrkDv3N	427 bp fragment amplified using pMrkDv3 as template and primer pairs, phw19 and phw07, and cloned into pET30a by <i>Sac</i> I and <i>Xho</i> I site, Kan ^r	This study
pMrkDV3NS	360 bp fragment amplified using pMrkDv3 as template and primer pairs, MZ007 and phw13, and cloned into pET30a by <i>Hind</i> III and <i>Xho</i> I site, Kan ^r	This study
pdMrkDV3NS	310 bp fragment amplified using pMrkDv3 as template and primer pairs, phw19 and phw13, and cloned into pET30a by <i>Sac</i> I and <i>Xho</i> I site, Kan ^r	This study
pdMrkB-1-pET	659 bp fragment amplified using <i>k. p</i> NTUH k2044 as template and primer pairs, phw22 and phw23, and	This study

pMrkF-YT	cloned into pET30a by <i>NdeI</i> and <i>NotI</i> site, Kan ^r 0.7 kb fragment amplified using primer pairs, phw15 and phw16, and cloned into yT&A cloning vector, Ap ^r	This study
pMrkF-pET	<i>mrkF</i> fragment digested from pMrkF-YT using <i>NcoI</i> and <i>HindIII</i> site and cloned into pET30a expression vector, Kan ^r	This study
pMrkABC	<i>mrkABC</i> gene cluster cloned into pGEMT vector, Ap ^r	72
pMrkABCD	1 kb fragment amplified using primer pairs, phw03 and MZ006, and cloned into pMrkABC by <i>AscI</i> and <i>ApaI</i> site, Ap ^r	This study
pMrkABCF	0.7 kb fragment amplified using primer pairs, F-N and F-C, and cloned into pMrkABC by <i>ApaI</i> site, Ap ^r	This study
pMrkABCDF	0.7 kb fragment amplified using primer pairs, F-N and F-C, and cloned into pMrkABCD by <i>ApaI</i> site, Ap ^r	This study



Table 3. Primers used in this study

Primer	Sequence 5' →3'	Enzyme site	Tm
phw03	CACCCTGTGGCGGCAAAAAA	<i>Dra</i> III site	60.3 °C
phw05	GCTATTTTGC GGCCGCCTCG	<i>Not</i> I site	63.3 °C
phw06	CGAGGCGGCCGCAA ATAGC	<i>Not</i> I site	63.3 °C
phw07	GGTGTATTTTCCCGC CTCGAGG	<i>Xho</i> I site	58.7 °C
phw12	GGAGCTCGAGACCAC GGTGAT	<i>Xho</i> I site	57.7 °C
phw13	CTCGAGACGAATAGA CGTCGGGA	<i>Xho</i> I site	59.2 °C
phw14	GAGCTCGAGTCGCATATGATCTT	<i>Sac</i> I site	54.4 °C
phw15	AGGGGCCATGGAGGGATT	<i>Nco</i> I site	55.2 °C
phw16	ATTATAAACTAGTTCCCACGTCGC	No	52.9 °C
phw19	GTCCTGGGAGCTCTGTACGCGC	<i>Sac</i> I site	61.9 °C
phw22	AGTTTTGC GGCCCATATGAA	<i>Nde</i> I site	54.6 °C
phw23	GCGGCCGCTTTC ACTGC	<i>Not</i> I site	57.5 °C
F-N	ATACGGGCCCGGGAATGAAGG	<i>Apa</i> I site	62.5 °C
F-C	TGAACA ACTGGGCCCGATGAT	<i>Apa</i> I site	62.0 °C
MZ006	GGGCCCTTAATCGTACGTCAGGTT	<i>Apa</i> I site	60.3 °C
MZ007	CAAGCTTTTATGAAAAA CTGACGCTTT	<i>Hind</i> III site	58.7 °C
MZ008	CTCGAGATCGTACGTCAGGTTAAA	<i>Xho</i> I site	54.4 °C

	1	10	20	30	40	51
mrkA	---MKKVLLSAAMATAFFGMTAAHAADTNVGGGQVNFPGKVTDVSC TVSVN					
mrkF	MKGLPKNTIAWLLFCGSLAAPSANGFETNYDRGRVDFAGRVTDISCSVALN					
Consensus	L K I A L A A A A DTN G V F GKVTDISCSVALN					

	52	60	70	80	90	102
mrkA	G--QGSDANVYLSPVTLTEVKAAAADTYLKPKSFTIDVSNCAAA-DG--TK					
mrkF	GGQHAGSGNVWLPVSLAEVHDRGAGAFMKPQPFTLALSNCQLRHDGGAAS					
Consensus	G A ANVWLPVSL EV AA FLKP FTI LSNCA DG					
	103	110	120	130	140	153
mrkA	QDDVSKLGVNWTGGNLLAGATSKQQGYLANTEASGAQNIQLVLSTDNATAL					
mrkF	QDEVRRVSVRWVDGFLLTAVGNENAGYLANTLPDGAQNIYLALSTNDNNTL					
Consensus	QDDV KL V W G LL A N GYLANT GAQNI L LST L					
	154	160	170	180	190	204
mrkA	T--NKIIPGDSTQPKAKGDASAVADGARFTYYVGYATSAPTTVTTGVVNSY					
mrkF	DKSNKIIVPADPQQNQVRLQESAVS-GGLFTYYVGYVSPTEPKSATSGPITSW					
Consensus	NKIIPAD Q K SAVA GA FTYYVGY S P S TSG I SW					
	205	213				
mrkA	ATYEITYQ-					
mrkF	ATWELVYN-					
Consensus	ATWEI YN					

Fig. 2. Amino acid sequence alignment of MrkA and MrkF. Alignment of MrkF amino acid sequence with MrkA showed MrkF has a conserved pilin domain as MrkA. The numbers on each section indicate the residues number of MrkF.



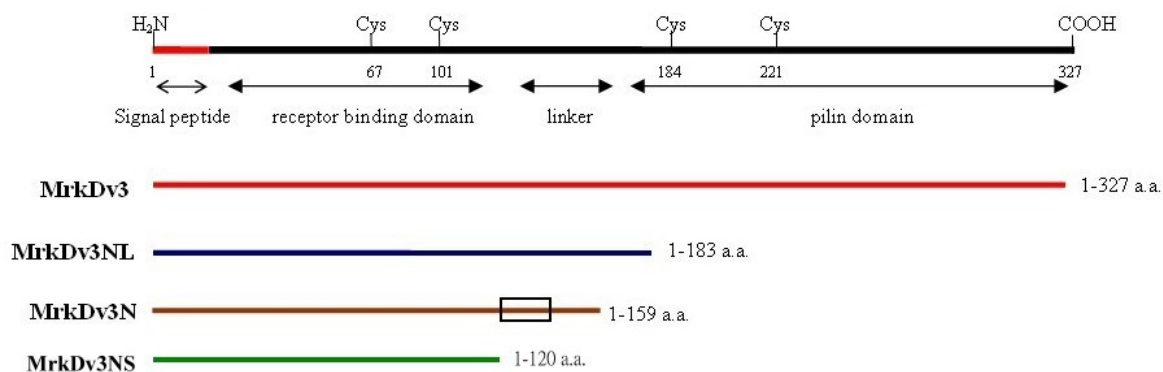


Fig. 3. Physical map of the recombinant proteins prepared in this study. The N-terminal receptor binding domain of MrkDv3 is responsible for binding activity and C-terminal pilin domain is responsible for assembly. The folding of each domain is stabilized by conserved cysteine residues. A linker is located between these two domains. The first twenty-two residues are signal peptides predicted by Clegg (34). The recombinant proteins, MrkDv3, MrkDv3NL, MrkDv3N and MrkDv3NS, are indicated by lines under the physical map. The rectangle marked on MrkDv3N indicates the position of the variable region, Gly₁₂₀ to Gln₁₄₀, on MrkDv3.



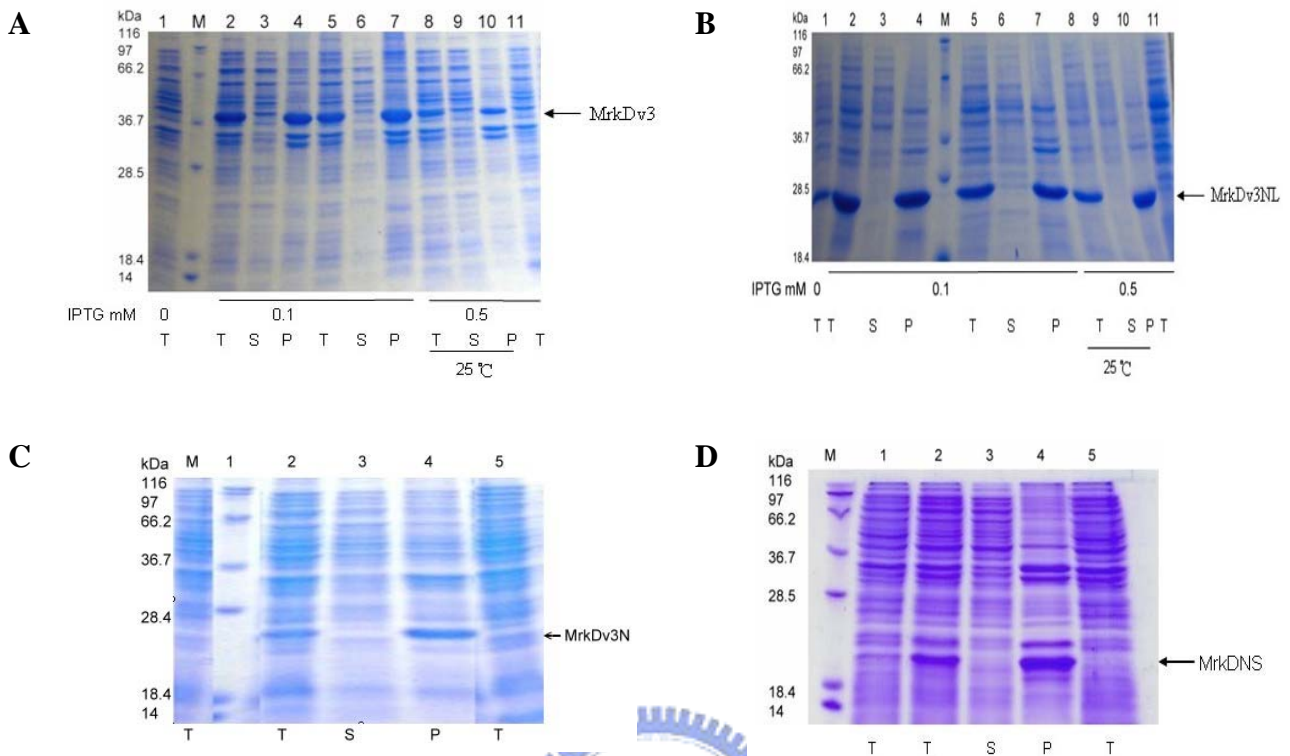


Fig. 4. SDS-PAGE analysis of the recombinant proteins. The arrows indicate the predicted recombinant proteins. The sample in each lane was prepared from the cells carrying each of the following plasmid: (A) pMrkDv3, (B) pMrkDv3NL, (C) pMrkDv3N, and (D) pMrkDv3NS. The culture condition is marked under pictures. Before loading, bacteria solution was sonicated twice for 30 seconds and centrifuged (13200 rpm, 10 min). T: total cell lysate; S: supernatant; P: pellet.

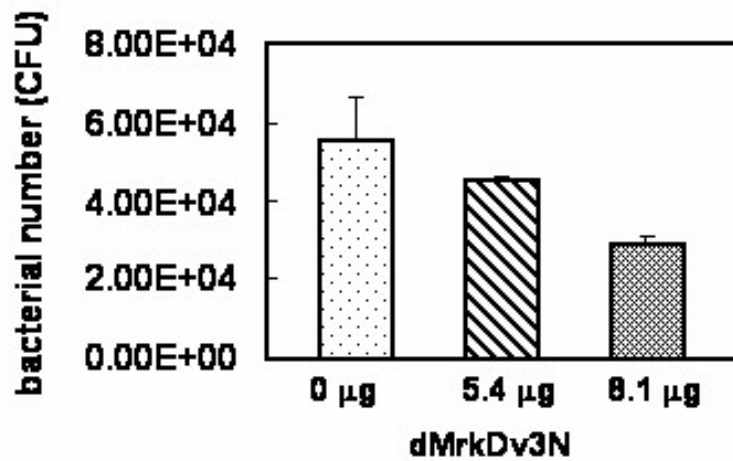


Fig. 5. Competition assay. dMrkDv3N was used as a competitor against *E. coli* carrying type 3 fimbriae with MrkDv3 in collagen IV binding assay. As increasing of the amount of dMrkDv3, the recovered bacteria decreased.



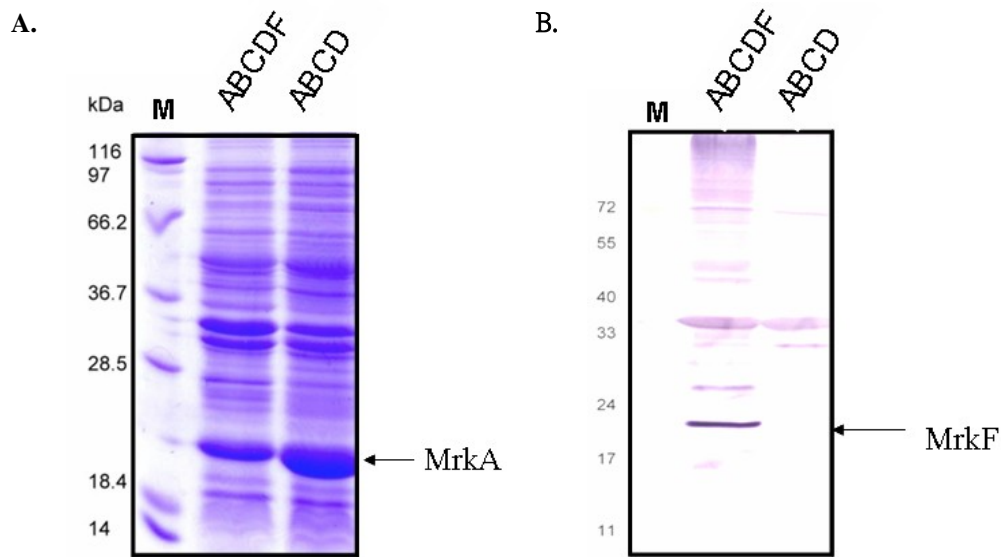


Fig. 6. Western blotting analysis of the recombinant *E. coli* displaying type 3 fimbriae. MrkF was expressed in *E. coli* and detected with anti MrkF antiserum. (A) SDS-PAGE separated recombinant *E. coli* lysates stained with Coomassie brilliant blue. (B) Western blotting analysis using anti MrkF antiserum.



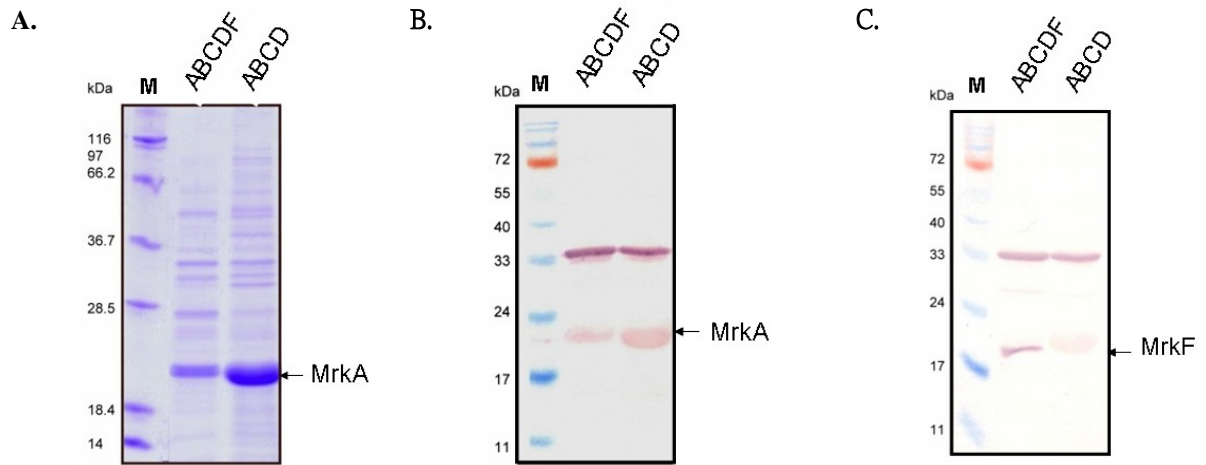


Fig. 7. Western blotting analysis of the purified type 3 fimbriae. MrkF protein was co-purified with, and strongly associated with type 3 fimbriae. (A) SDS-PAGE separated type 3 fimbriae stained with Coomassie brilliant blue. (B) Western blotting analysis using anti MrkA antiserum. (C) Western blotting analysis using anti MrkF antiserum.



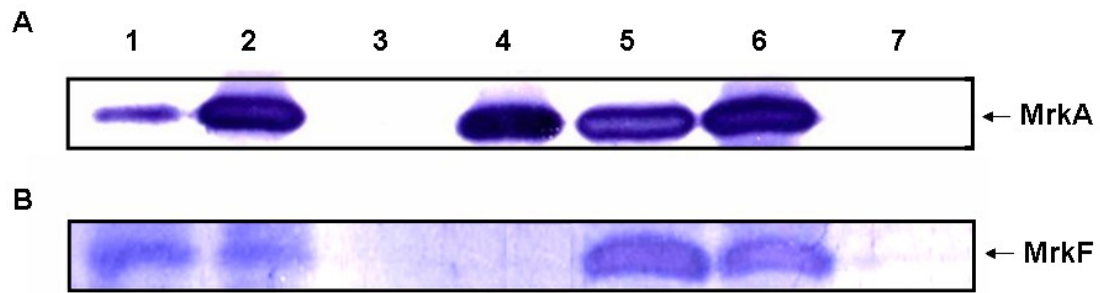


Fig. 8. Co-immunoprecipitation. Co-immunoprecipitation studies with anti-MrkA and anti-MrkF antisera. The purified fimbriae of *E. coli* JM109[pmrkABCDF] (lane 1, 2), JM109[pmrkABCD] (lane 3, 4) and JM109[pmrkABCF] (lane 5, 6) were precipitated with anti MrkF antibody (odd lane) and anti MrkA antibody (even lane). The purified fimbriae of *E. coli* JM109[pmrkABCDF] not added antibody as negative control (lane 7). The blots were then probed with antiserum to the MrkA (A) and MrkF (B) proteins listed at the right.



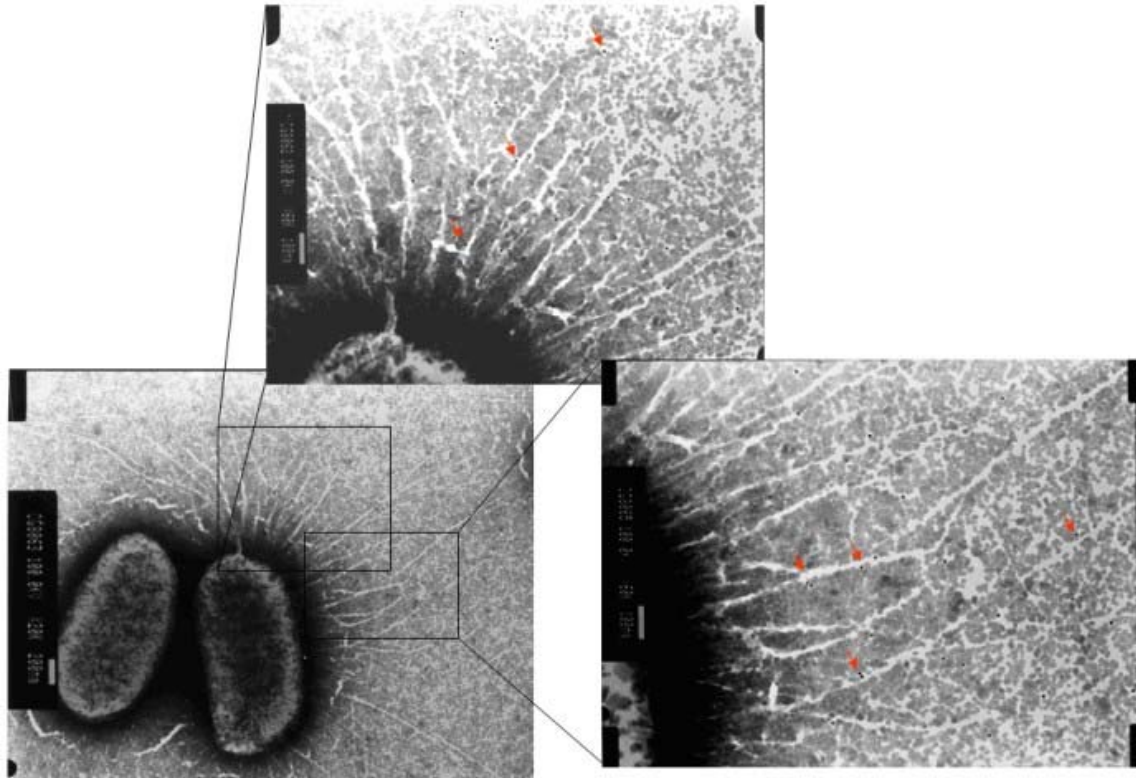


Fig. 9. Electron micrographs of the anti-MrkF immuno-gold labeled pili. Labeling was against the minor subunit MrkF. The antibody distributed in the pilus rod by several copies. The magnified views showed the position of MrkF in type 3 fimbraie. The gold size was 10 nm. The scale bars represent: 200 nm in the picture with whole bacteria; and 100 nm in the other two pictures.

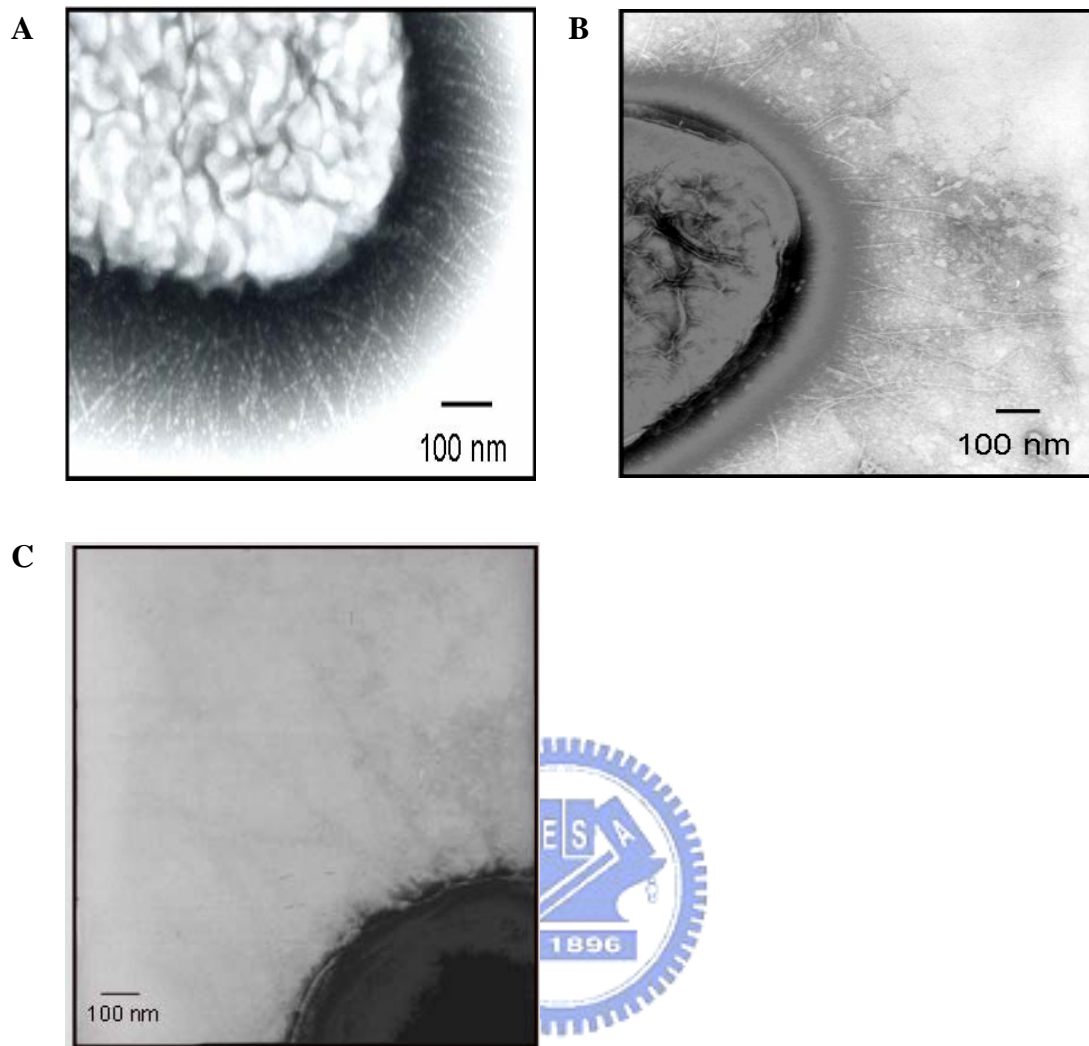


Fig. 10. Electron micrographs of the recombinant *E. coli*. (A) HB101[pmrkABCDF], (B) HB101[pmrkABCD] and (C) HB101[pmrkABCF] were negatively stained with 2 % phosphotungstic acid and imaged by TEM. The type 3 pili are clearly visible and fimbrial morphology including amount and length is quite variable.

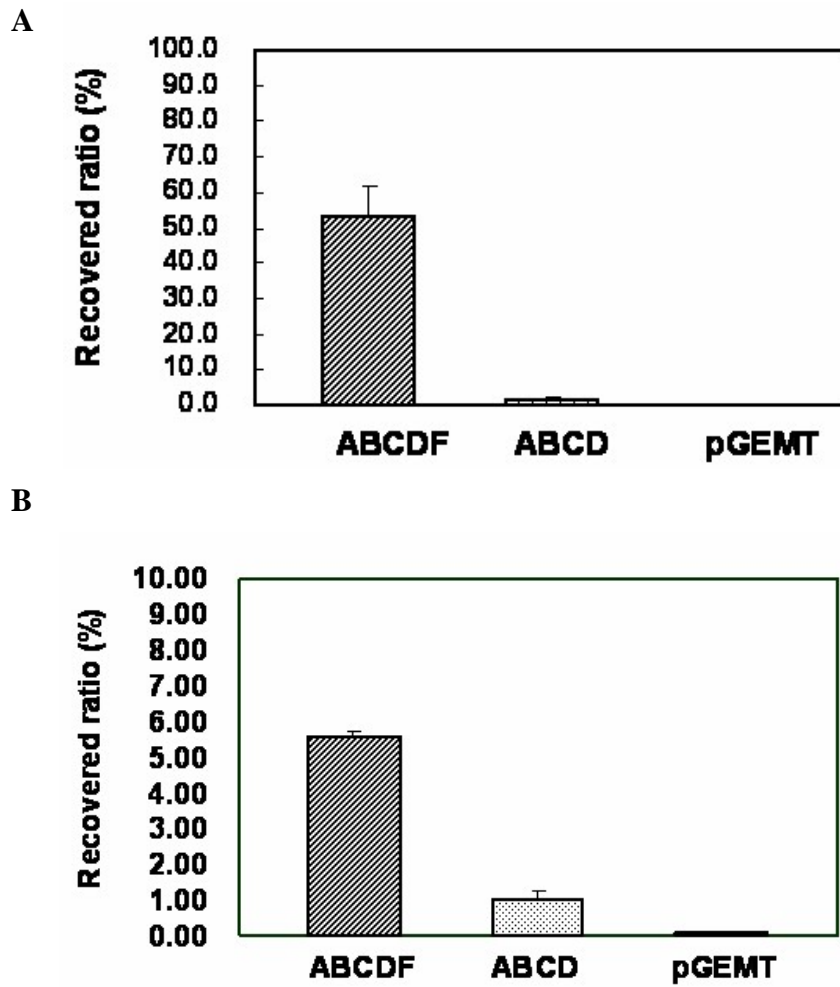


Fig. 11. Collagen binding activity of the recombinant *E. coli*. The recovered bacteria were indicated as recovered percentage. Each bacterium is marked by its expression plasmid. (A) collagen IV binding assay and (B) collagen V binding assay.

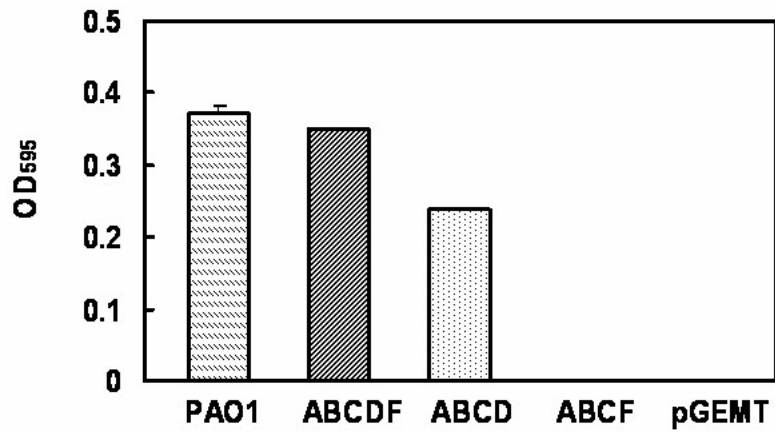


Fig. 12. Biofilm formation of the recombinant *E. coli*. Each bacterium is indicated by its expression plasmid. Results are expressed as the average of three independent experiments (5 standard deviation). Quantification of biofilm formation was determined by the absorbance of OD₅₉₅ for each of the *E. coli* variants.



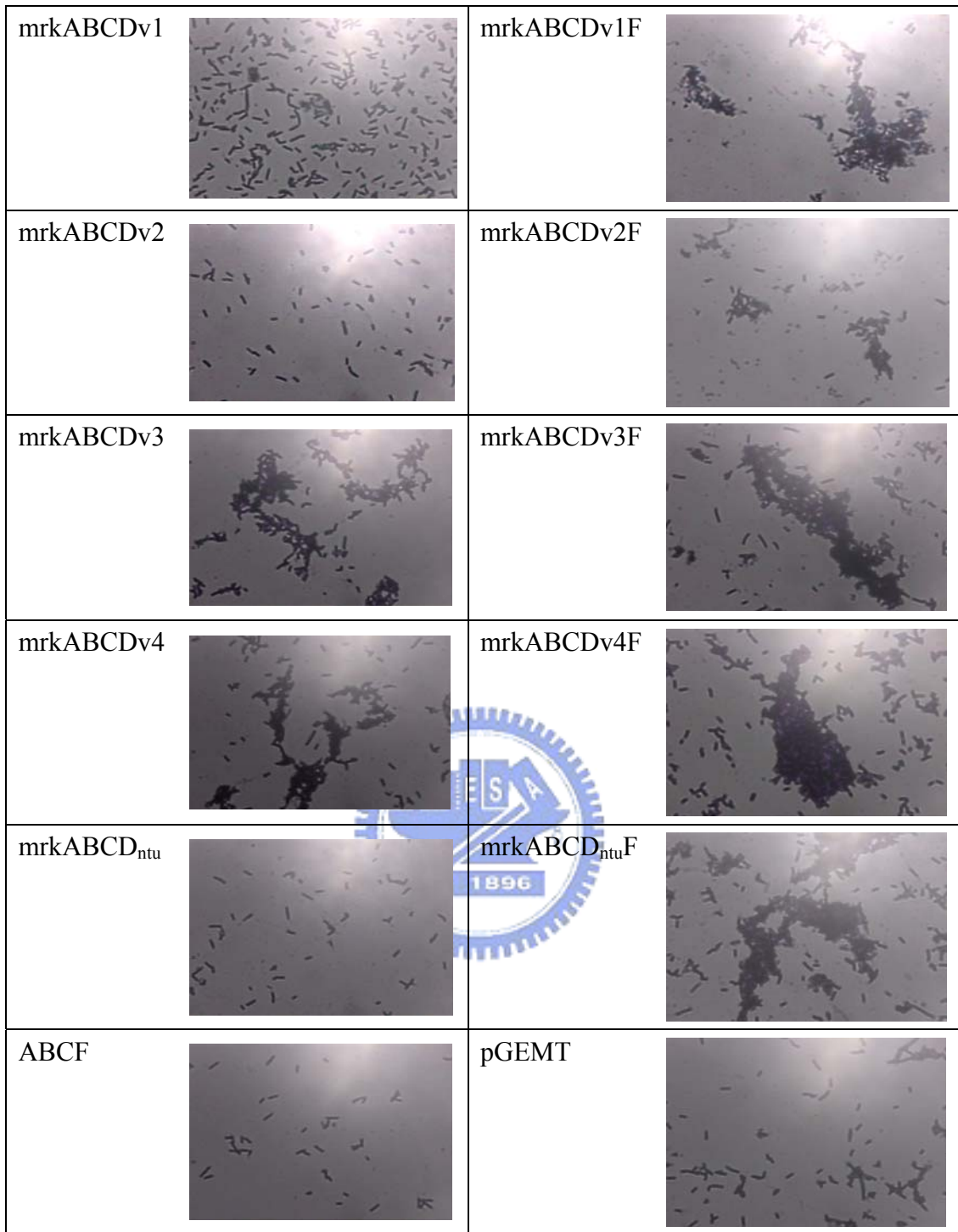


Fig. 13. Autoaggregative phenotypes. Light microscopy demonstrating the autoaggregative phenotype of recombinant JM109 expressing MrkD variants. As a control, the phenotype of bacteria transformed with vector only or pMrkABCF are also shown. The effect of MrkF on autoaggregation was assessed by comparing phenotypes of *E. coli* with or without MrkF.